

ISTANBUL TECHNICAL UNIVERISTY

FINAL PROJECT

Design of Extended Kalman Filters for Estimation of UAV Flight Parameters

Author:

Carlos CARAVACA

Supervisor:

Cengiz HACIZADE

Higher Technical School of
Engineering of Seville
University of Seville
Seville, 41092, Spain

Faculty of Aeronautics and
Astronautics
Istanbul Technical University
Maslak, 34469, Istanbul,
Turkey

Faculty of Aeronautics and
Astronautics
Istanbul Technical University
Maslak, 34469, Istanbul,
Turkey

cingiz@itu.edu.tr

carcargal1@alum.us.es

*A project submitted in fulfillment of the requirements
for the degree of Aerospace Engineering*

in the

Department of Aeronautical Engineering

July 13, 2020

Declaration of Authorship

I, Carlos CARAVACA, declare that this thesis titled, "Design of Extended Kalman Filters for Estimation of UAV Flight Parameters" and the work presented in it are my own. I confirm that:

- This work was done wholly or mainly while in candidature for a degree at this University.
- Where any part of this thesis has previously been submitted for a degree or any other qualification at this University or any other institution, this has been clearly stated.
- Where I have consulted the published work of others, this is always clearly attributed.
- Where I have quoted from the work of others, the source is always given. With the exception of such quotations, this thesis is entirely my own work.
- I have acknowledged all main sources of help.
- Where the thesis is based on work done by myself jointly with others, I have made clear exactly what was done by others and what I have contributed myself.

Signed:

Date:

“If one day my words are against science, choose science.”

Mustafa Kemal Atatürk

ISTANBUL TECHNICAL UNIVERISTY

Abstract

Faculty of Aeronautics and Astronautics
Department of Aeronautical Engineering

Aerospace Engineering

Design of Extended Kalman Filters for Estimation of UAV Flight Parameters

by Carlos CARAVACA

In this research the derivation of UAV mathematical model and the estimation of the aircraft flight parameters using Extended Kalman Filtering technique are investigated. For this purpose, a simulation of the UAV sensor measurements is carried out and the Extended Kalman Filter is designed. Finally, the velocity components, angle of attack and sideslip angle are estimated. In the last part of the project, a fault detection algorithm based on the innovation step of the Kalman Filter is derived and tested to unmask potential malfunctioning of the sensor measurements, which is indispensable to flight safety.

Acknowledgements

First and foremost I would like to thank my supervisor Prof. Dr. Cengiz Hacizade for his dedicated involvement in every step of the development of this project, without his assistance this paper would have never been completed. I would also like to express gratitude to my Erasmus coordinators and every person involved in the realization of my Erasmus mobility, both at Istanbul Technical University and at University of Seville, specially during this historic year of global crisis where so many adjustments were needed. Most importantly, none of this could have happened without my friends and my family, both of which grew in number during my stay in Istanbul.

Contents

Declaration of Authorship	iii
Abstract	vii
Acknowledgements	ix
1 Introduction	1
2 Problem Formulation	3
3 Mathematical Model of UAV	5
4 Extended Kalman Filter for UAV State Estimation	7
4.1 Definition of EKF	7
4.2 EKF Simulation Results	8
4.3 Flight Parameters Measurements	9
5 EKF Based Sensor Fault Detection	11
5.1 Fault Detection Algorithm	11
5.2 Sensor Fault Detection Simulation Results	12
6 Conclusion	17
Bibliography	19

List of Figures

4.1	EKF estimation of velocity components and variance of estimation error	8
4.2	Innovation vector components	9
5.1	Fault Detection Algorithm Results	13
5.2	EKF estimation of velocity components and variance of estimation error in the presence of u velocity component bias	14
5.3	Innovation vector components in the presence of u velocity component bias	14
5.4	EKF estimation of velocity components and variance of estimation error in the presence of alpha bias	15
5.5	Innovation vector components in the presence of alpha bias	15
5.6	EKF estimation of velocity components and variance of estimation error in the presence of beta bias	16
5.7	Innovation vector components in the presence of beta bias	16

List of Tables

4.1 Discrete Extended Kalman Filter	7
-----------------------------------------------	---

List of Abbreviations

UAV	Unmanned Aerial Vehicle
EKF	Extended Kalman Filter
AOA	Angle Of Attack
AOS	Angle Of Sideslip
ADS	Air Data System
KF	Kalman Filter
IMU	Inertial Measurement Unit
SWS	Stall Warning System
NN	Neural Network
UKF	Unscented Kalman Filter

Chapter 1

Introduction

The estimation of flight parameters, namely, the velocity components and the angle of attack and sideslip, is essential to safe flight control since a number of critical systems, such as stall warning system (SWS) and indications of surrounding air flows, rely heavily on these values [1]. Therefore, the lack of accuracy in the calculation of these variables may lead to catastrophic consequences, hence the need for redundancy of the aforementioned signals. This can be achieved by the integration of different types of measures through the application of the Kalman Filter algorithm, which is an efficient recursive filter that estimates the internal state of a dynamic system from a series of noisy measurements [2]. In this case, both direct measurement through sensors installed on the aircraft as well as inertial estimation via the Inertial Measurement Unit (IMU) are used for this purpose (see section 4.3). On the other hand, since a non-linear approach is being applied, the employment of the Extended Kalman Filter (EKF) is needed. This variation linearizes about an estimate of the current mean and covariance and has been considered the actual standard [3] in the theory of nonlinear state estimation (see section 4.1).

In addition, the application of the EKF can also behave as a tool in order to detect faults that can affect the sensor network. After this detection, which is carried out by comparing a statistical function against a threshold (see section 5.1), the next step is naturally the design of algorithms to isolate this faulty measure and prevent it from influencing the actual measure, which is critical as it was stated in the previous paragraph. Nevertheless, despite the fact that fault detection is to be analyzed, the isolation of faults is not to be covered in this paper, given the main objective is the study and design of the EKF itself. On the topic of fault isolation, Caliskan and Hajiyev (2014) [4] made an approach to isolate the sensor and actuator failures affecting the innovation of the Kalman Filter, and it was applied to an UAV dynamic model.

Furthermore, several studies have been carried out with respect to these techniques; namely, Hajiyev and Caliskan (2003) [5] introduced a comprehensive research of fault diagnosis and reconfigurable control. The methods investigated are based on linear and nonlinear dynamic mathematical models, observers and KF. Besides, Hajiyev and Caliskan (2005) [6] presented an approach to detect and isolate aircraft sensor and actuator faults. Additionally, Soken et al. (2014) [7] proposed an adjustment of EKF and unscented Kalman filter (UKF) algorithms for attitude estimation of a small satellite. These modifications upgraded the filters, which became robust against measurement malfunctions. They used a multiple scale factor based scheme for adapting the filters, hence the prevention of any unnecessary information loss since only the data of the faulty sensor is corrected. Finally, Cork et al. (2005) [8] presented the results obtained from a fault detection scheme that identified the critical failures of the angular rate sensors from an unmanned aerial vehicle

(UAV) using a neural network (NN), which is integrated altogether with the KF to obtain better results. In fact, Caliskan and Hajiyeve (2013) [9] studied the combined case for aircraft icing identification. In this undergraduated thesis the estimation of UAV states and Kalman filter based sensor fault detection applied to UAV model of dynamics are investigated.

Chapter 2

Problem Formulation

Firstly, a mathematical model of the UAV is needed in order to simulate the motion of the aircraft, as well as the measurements required to apply the Kalman Filter. This model, which will be simulated through Matlab, is explained in Chapter 3. After the simulations of the motion of the aircraft and the sensor measurements are carried out, the Kalman Filter algorithm is to be applied, which will integrate both measures resulting in a more reliable estimate of the actual flight parameters of the UAV. By using the body-axis velocity components, angles of attack and sideslip can be calculated as follows:

$$\alpha = \arctan\left(\frac{w}{u}\right) \quad (2.1)$$

$$\beta = \arcsin\left(\frac{v}{\sqrt{u^2 + v^2 + w^2}}\right) \quad (2.2)$$

Also, the state equation and measurement equations can be defined in this way:

$$x(k+1) = \phi(k+1, k)x(k) + G(k+1, k)w(k) \quad (2.3)$$

$$z(k) = H(k)x(k) + v(k) \quad (2.4)$$

where $x(k)$ is n dimensional state vector of the system, $\phi(k+1, k)$ is $n \times n$ dimensional transition matrix of the system, $w(k)$ is n dimensional random system noise, $G(k+1, k)$ is $n \times n$ dimensional transition matrix of system noise, $z(k)$ is s dimensional measurement vector, $H(k)$ is $s \times n$ dimensional measurement matrix of the system and $v(k)$ is s dimensional random measurement noise vector.

In Chapter 5.1 it will be shown that in the application of the Kalman Filter to this dynamic system, the innovation step and its statistical properties can be used to detect faults in the sensor measurements system.

Chapter 3

Mathematical Model of UAV

In order to build a Kalman filter for the state estimation of an UAV, the characteristics of the flight dynamics must be known. For this purpose, the general approach is to derive the rigid body equations of motion and then linearize them by applying the small disturbance theory [10]. These linearized equations are divided in longitudinal and lateral equations and discretized as follows [11]:

$$\mathbf{x}^{lon}(k+1) = \mathbf{A}^{lon}\mathbf{x}^{lon}(k) + \mathbf{B}^{lon}\mathbf{u}^{lon}(k) \quad (3.1)$$

$$\mathbf{x}^{lat}(k+1) = \mathbf{A}^{lat}\mathbf{x}^{lat}(k) + \mathbf{B}^{lat}\mathbf{u}^{lat}(k) \quad (3.2)$$

where the state vectors $\mathbf{x}^{lon}(k)$ and $\mathbf{x}^{lat}(k)$ and control vectors $\mathbf{u}^{lon}(k)$ and $\mathbf{u}^{lat}(k)$ are given by

$$\mathbf{x}^{lon}(k) = \begin{bmatrix} \Delta u \\ \Delta w \\ \Delta q \\ \Delta \theta \\ \Delta h \end{bmatrix}_k; \mathbf{x}^{lat}(k) = \begin{bmatrix} \Delta \beta \\ \Delta p \\ \Delta r \\ \Delta \phi \end{bmatrix}_k; \mathbf{u}^{lon}(k) = \begin{bmatrix} \Delta \delta_e \\ \Delta \delta_T \end{bmatrix}_k; \mathbf{u}^{lat}(k) = \begin{bmatrix} \Delta \delta_a \\ \Delta \delta_r \end{bmatrix}_k \quad (3.3)$$

and the matrices \mathbf{A}^{lon} , \mathbf{B}^{lon} , \mathbf{A}^{lat} and \mathbf{B}^{lat} are given by

$$\mathbf{A}^{lon} = \begin{bmatrix} X_u & X_w & 0 & -g & 0 \\ Z_u & Z_w & u_0 & 0 & 0 \\ M_u + M_{iw}Z_u & M_w + M_{iw}Z_w & M_q + M_{iw}u_0 & 0 & 0 \\ 0 & 0 & 1 & 0 & 0 \\ 0 & -1 & 0 & u_0 & 0 \end{bmatrix} \quad (3.4)$$

$$\mathbf{B}^{lon} = \begin{bmatrix} X_{\delta_e} & X_{\delta_T} \\ Z_{\delta_e} & Z_{\delta_T} \\ M_{\delta_e} + M_{iw}Z_{\delta_e} & M_{\delta_T} + M_{iw}Z_{\delta_T} \\ 0 & 0 \\ 0 & 0 \end{bmatrix} \quad (3.5)$$

$$\mathbf{A}^{lat} = \begin{bmatrix} \frac{Y_{\beta}}{u_0} & \frac{Y_p}{u_0} & -\frac{u_0 - Y_r}{u_0} & \frac{g \cos(\theta_0)}{u_0} \\ L_{\beta} & L_p & L_r & 0 \\ N_{\beta} & N_p & N_r & 0 \\ 0 & 1 & 0 & 0 \end{bmatrix} \quad (3.6)$$

$$\mathbf{B}^{lat} = \begin{bmatrix} 0 & \frac{Y_{\delta r}}{u_0} \\ L_{\delta a} & L_{\delta r} \\ N_{\delta a} & N_{\delta r} \\ 0 & 0 \end{bmatrix} \quad (3.7)$$

On the other hand, the state equations described in terms of the velocity components (u, v, w) , the angular rates (p, q, r) and the roll ϕ and pitch θ attitude angles are shown below:

$$\dot{u} = A_{x_m} - q_m w + r_m v - g \sin(\theta) \quad (3.8)$$

$$\dot{v} = A_{y_m} - r_m u + p_m w + g \sin(\phi) \cos(\theta) \quad (3.9)$$

$$\dot{w} = A_{z_m} - p_m v + q_m u + g \cos(\phi) \cos(\theta) \quad (3.10)$$

$$\dot{\phi} = p_m + q_m \sin(\phi) \tan(\theta) + r_m \cos(\phi) \tan(\theta) \quad (3.11)$$

$$\dot{\theta} = q_m \cos(\phi) - r_m \sin(\phi) \quad (3.12)$$

$$\dot{h} = u \sin(\theta) - v \sin(\phi) \cos(\theta) - w \cos(\phi) \cos(\theta) \quad (3.13)$$

Chapter 4

Extended Kalman Filter for UAV State Estimation

4.1 Definition of EKF

The existence of a large number of different estimation problems involving non-linear models requires the application of the EKF, which is the variation of the Kalman Filter that linearizes about an estimate of the current mean and covariance . There are a number of reasons why state estimation is a considerably more difficult problem for non-linear systems admitting a much wider variety of solutions than the linear version of the problem [12]. In essence, the fundamental concept behind the successful implementation of this variation is the assumption of the true state being close enough to the estimated state, thus error dynamics can be represented accurately enough by a linearized first-order Taylor series expansion [13]. Nevertheless, this restriction may be harmful for deeply nonlinear applications with large initial condition errors and convergence for this algorithm is rather difficult to prove even for simple systems [14]. Fortunately, the EKF is, in general, robust to initial condition errors (this can be verified through simulation).

TABLE 4.1: Discrete Extended Kalman Filter

Model	$\dot{\mathbf{x}}(t) = \mathbf{f}(\mathbf{x}(t), \mathbf{u}(t), t) + G(t)\mathbf{w}(t), \mathbf{w}(t) \sim N(\mathbf{0}, Q(t))$ $\tilde{\mathbf{y}}_k = \mathbf{h}(\mathbf{x}_k) + \mathbf{v}_k, \mathbf{v}_k \sim N(\mathbf{0}, R_k)$
Initialize	$\hat{\mathbf{x}}(t_0) = \hat{\mathbf{x}}_0$ $P_0 = E \{ \tilde{\mathbf{x}}(t_0) \tilde{\mathbf{x}}^T(t_0) \}$
Gain	$K_k = P_k^- H_k^T(\hat{\mathbf{x}}_k^-) [H_k(\hat{\mathbf{x}}_k^-) P_k^- H_k^T(\hat{\mathbf{x}}_k^-) + R_k]^{-1}$ $H_k(\hat{\mathbf{x}}_k^-) \equiv \left. \frac{\partial \mathbf{h}}{\partial \mathbf{x}} \right _{\hat{\mathbf{x}}_k^-}$
Update	$\hat{\mathbf{x}}_k^+ = \hat{\mathbf{x}}_k^- + K_k [\tilde{\mathbf{y}}_k - \mathbf{h}(\hat{\mathbf{x}}_k^-)]$ $P_k^+ = [I - K_k H_k(\hat{\mathbf{x}}_k^-)] P_k^-$
Propagation	$\hat{\mathbf{x}}(t) = \mathbf{f}(\hat{\mathbf{x}}(t), \mathbf{u}(t), t)$ $\dot{P}(t) = F(\hat{\mathbf{x}}(t), t) P(t) + P(t) F^T(\hat{\mathbf{x}}(t), t) + G(t) Q(t) G^T(t)$ $F(\hat{\mathbf{x}}(t), t) \equiv \left. \frac{\partial \mathbf{f}}{\partial \mathbf{x}} \right _{\hat{\mathbf{x}}(t)}$

Table 4.1 summarizes the discrete version of the EKF [13]. In this table, $x(t)$ represents the state vector, $u(t)$ the input vector, $w(t)$ the random system or model error (assumed to be a zero-mean Gaussian white-noise process), $G(t)$ the operator which maps this error into state space, \tilde{y}_k the measurement model, v_k the measurement error (also a zero-mean Gaussian white-noise process uncorrelated to $w(t)$), P_0 the initial error-variance, K_k the Kalman gain, P_k^- the covariance update, H_k the observation model which maps the true state space into the observed space, R_k the covariance of the observation noise, P_k^+ the *a posteriori* estimate covariance matrix, and finally I is the identity matrix.

4.2 EKF Simulation Results

After the problem has been formulated and the EKF algorithm defined, its adequate operation will be tested in this Chapter. A Matlab program has been designed both to simulate the motion of the UAV according to the mathematical model proposed in Chapter 3, as well as to reproduce the functioning of the EKF.

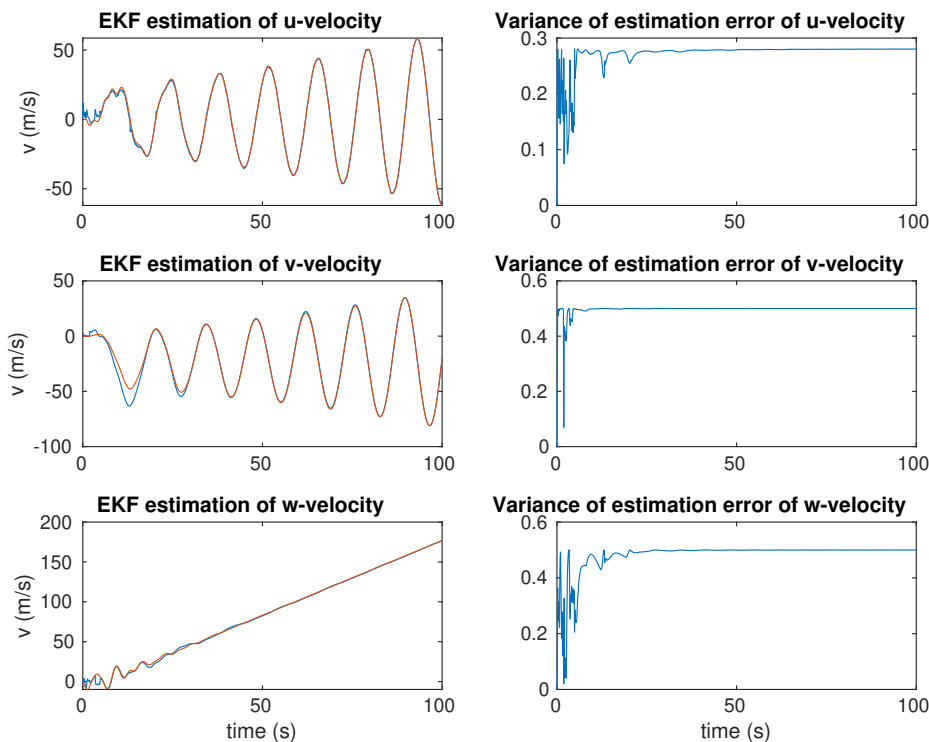


FIGURE 4.1: EKF estimation of velocity components and variance of estimation error

On the other hand, it is important to mention that the chosen model of UAV is unstable and control algorithm is not applied, therefore oscillations and unstable flight may characterize the simulation results. Although introducing PID control or other control algorithm can remove these effects, this was not carried out since it does not affect the operation of the EKF nor the fault detection algorithm. Low initial values of control inputs were chosen in order to reduce these undesired effect.

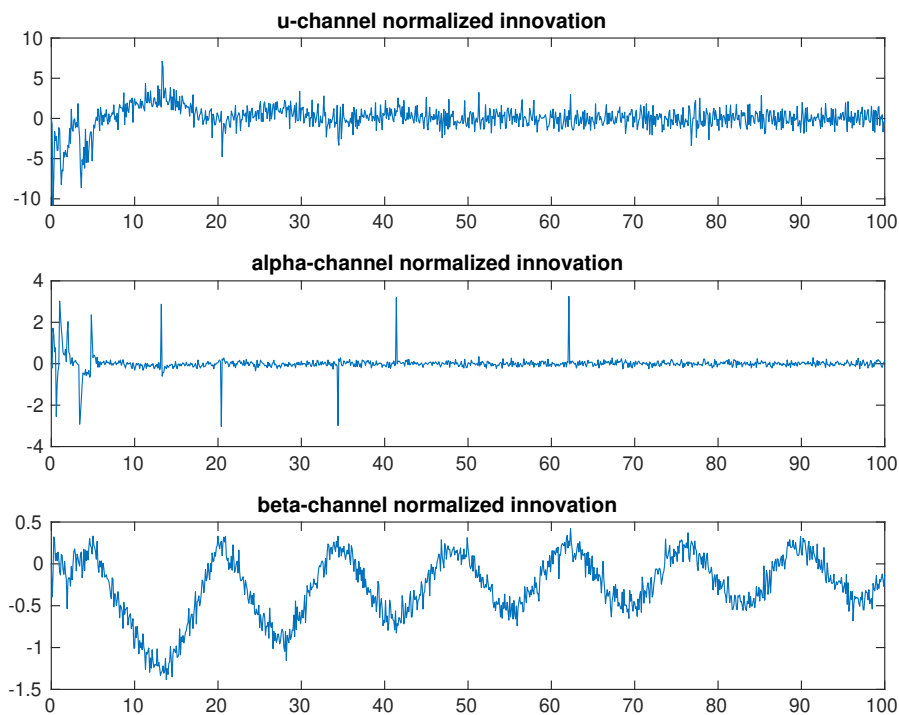


FIGURE 4.2: Innovation vector components

Figure 4.1 shows that in fact, the EKF is operating to an acceptable standard, being able to closely approximate (EKF estimation is represented in blue) the true state of the aircraft (represented in orange) despite the oscillations in the velocity components. It is also interesting to mention that the algorithm behaves more poorly in the early stages of the application, due to the approximation of the non linear model to a linearized first-order Taylor series expansion. As it was stated, it can be observed through simulation that although this variation can be significant at first, the algorithm is in general robust to this initial condition error, and eventually tends to converge. Figure 4.2 represents the components of the innovation vector of the EKF, computed as the difference between the actual measurements and the predicted measurements.

4.3 Flight Parameters Measurements

The measurement of flight data is essential in order to apply the Kalman Filter algorithm, therefore it is significant to analyze the various ways to achieve this. There are a number of methods by which AOA and AOS can be directly measured using sensors installed on an aircraft. The most common form of these sensors are multihole pitot tubes and flow vanes, which are mass-balanced wind vanes that align themselves with the direction of the approaching air flow [15]. A potentiometer determines the angle between the flow vane and the aircraft reference line. Although this is the most common method to determine these flight parameters directly, different alternatives can be used for this purpose, such as differential pressure probes [16], distributed flushed ADSs [17] and optical sensors [18].

For direct flow measurements are usually corrupted by noises, inertial AOA and AOS estimation methods are used, that is, this information is reconstructed using data from the pitot tube, accelerometers and gyroscopes. Even though both measured and inertial values typically match, local turbulences may arise differences [19], which is why the integration of the Kalman filter provides protection against malfunctioning of either of these two approaches for the determination of flight parameters.

Chapter 5

EKF Based Sensor Fault Detection

5.1 Fault Detection Algorithm

The innovation step is defined as the calculation of the difference between the actual system output and the predicted output based on the predicted state and it represents the new information contributed by the latest observation vector. Under faultless conditions, the error signal is relatively small and corresponds to random fluctuations in the output where all the systematic trends are eliminated by the model. However, under faulty conditions, the error signal is large and contains systematic trends since the model no longer represents the physical system adequately. First, we define the measurement innovation vector:

$$\Delta(k) = z(k) - H(k)\hat{x}(k/k-1) \quad (5.1)$$

where $\hat{x}(k/k-1)$ is the prediction in one step. If the system operates normally, then this innovation vector will behave as white Gaussian noise with zero mean and covariance matrix of:

$$P_{\Delta}(k) = H(k)P(k/k-1)H^T(k) + R(k) \quad (5.2)$$

In this equation, $P(k/k-1)$ is defined as:

$$P(k/k-1) = \phi(k,k-1)P(k-1/k-1)\phi^T(k,k-1) + G(k,k-1)Q(k-1)G^T(k,k-1) \quad (5.3)$$

which is the covariance matrix of extrapolation errors where $P(k-1,k-1)$ is the covariance matrix of estimation errors in the previous step. The estimated value of state vector $\hat{x}(k/k)$ and the covariance matrix of the estimation error $P(k/k)$ can be found by the KF as given:

$$\hat{x}(k/k) = \hat{x}(k/k-1) + K(k)\Delta(k) \quad (5.4)$$

$$K(k) = P(k/k-1)H^T(k) \left[H(k)P(k/k-1)H^T(k) + R(k) \right]^{-1} \quad (5.5)$$

$$P(k/k) = [I - K(k)H(k)] P(k/k-1) \quad (5.6)$$

where $K(k)$ is the Kalman Filter gain matrix and I is the unit matrix. On the other hand, it is more appropriate to use normalized innovation to detect the faults:

$$\tilde{\Delta}(k) = \left[H(k)P(k/k-1)H^T(k) + R(k) \right]^{-1/2} \Delta(k) \quad (5.7)$$

because in this case:

$$E \left[\tilde{\Delta}(k) \tilde{\Delta}^T(j) \right] = P_{\tilde{\Delta}} = I \delta(kj) \quad (5.8)$$

These faults of measurement sensors affect the characteristics of the normalized innovation vector by changing its white noise nature, displacing its zero mean and varying the unit covariance matrix, which has been encountered in the derivation of the Kalman filter measurement update as well. Thus, the problem is to detect any change in these parameters from their nominal value as quickly as possible. The innovation covariance has been encountered in the derivation of the Kalman filter measurement update as well and thus it can be seen that the innovation is an integral part of the Kalman filter process. The general performance of the filter can be monitored by analysing the zero mean, Gaussianness, given covariance and whiteness of the innovation sequence. Furthermore the innovation is the sole source of outlier detection.

$$\beta(k) = \tilde{\Delta}^T(k) \tilde{\Delta}(k) \quad (5.9)$$

These functions have χ^2 distribution with s degree of freedom, where s is the dimension of the innovation vector. If the level of significance, α , is selected as:

$$P \{ \chi^2 > \chi_{\alpha,z}^2 \} = \alpha; 0 < \alpha < 1 \quad (5.10)$$

Then the threshold value, $\chi_{\alpha,z}^2$, can be found using the chi-square distribution. Consequently, when the hypothesis γ_1 is true, the value of the statistical function $\beta(k)$ will be greater than the threshold value, $\chi_{\alpha,s}^2$, i.e.:

$$\gamma_0 : \beta(k) \leq \chi_{\alpha,s}^2 \quad \forall k \quad (5.11)$$

$$\gamma_1 : \beta(k) > \chi_{\alpha,s}^2 \quad \exists k \quad (5.12)$$

5.2 Sensor Fault Detection Simulation Results

In this chapter, the correct functioning of the the fault detection algorithm will be tested. The threshold value, $\chi_{\alpha,z}^2$, will be selected using the chi-square distribution with parameters: degrees of freedom $df = 3$ and probability $p = 0.99$. For this parameters, the corresponding χ^2 is equal to 11.34. This value will be used as the threshold value for the fault detection algorithm, and any value satisfying hypothesis γ_1 aforementioned in Chapter 5.1 will be considered as a fault signal.

All of the four scenarios which will be taken into consideration are displayed in Figure 5.1, where the red line represents the threshold selected and the blue line represents the statistical function $\beta(k)$. In the faultless scenario, it can be observed that due to the high magnitude of the noise involved in the early stages of the application of the EKF, $\beta(k)$ exceeds the threshold value. However, this should not be a problem if we only consider those situations where the threshold value is exceeded continuously rather than a one-time exception as the ones present in the faultless scenario. Moving on to the faulty scenarios, that is, where a bias is introduced either in the velocity components or in the AOA and AOS sensors, two different frameworks are presented; namely, where a velocity bias is introduced, the statistical function begins to detect a linearly ascending noise, whilst in the angles bias, $\beta(k)$ immediately

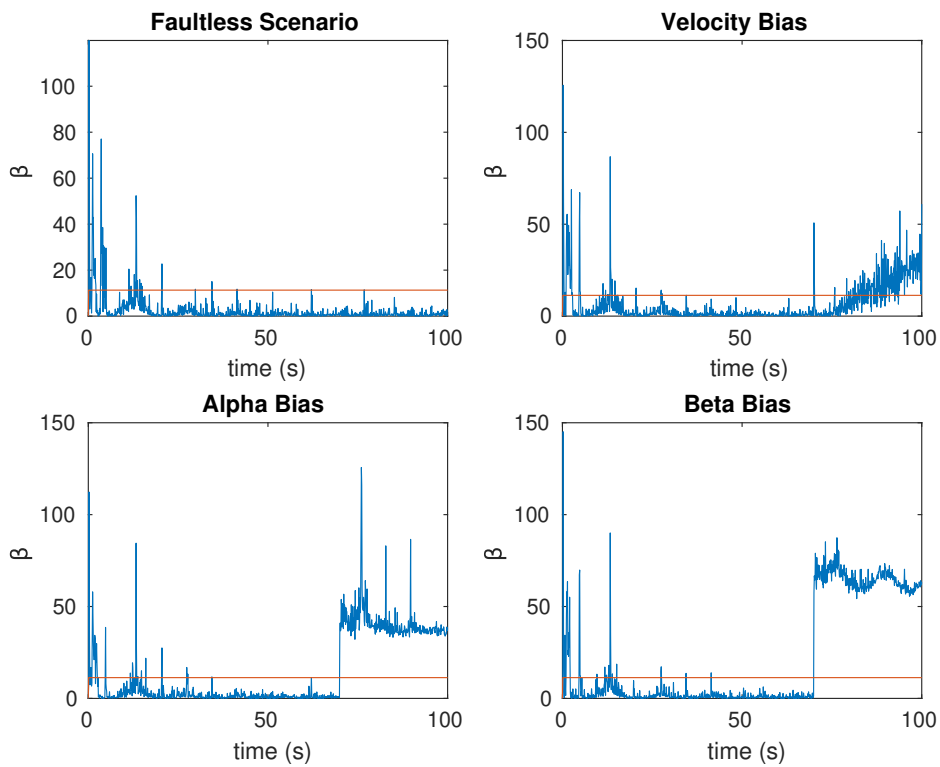


FIGURE 5.1: Fault Detection Algorithm Results

jumps far above the threshold line and oscillates around higher values. Thus, it is proven that the scenarios that satisfy hypothesis γ_1 can be easily detected through the innovation step of the EKF and it is both a reliable technique as well as significant (robust against false positive) if the exceptions due to initial condition errors are omitted and only those cases where the threshold is constantly exceeded.

The functioning of the EKF in the presence of u-velocity component bias, alpha bias and beta bias is represented in Figures 5.2, 5.4 and 5.6 where the approximation of the v and w components of the velocity are severely deteriorated after the bias is introduced at $t = 70s$. The effects of the introduction of the sensor fault can be easily observed in Figures 5.3, 5.5 and 5.7 where the u, alpha and beta channel clearly displays the appearance of the bias that triggers the fault detection algorithm. It is shown that alpha and beta channels display a step function immediately when the bias is introduced whereas the u-channel depicts a linear increasing function once the fault is triggered.

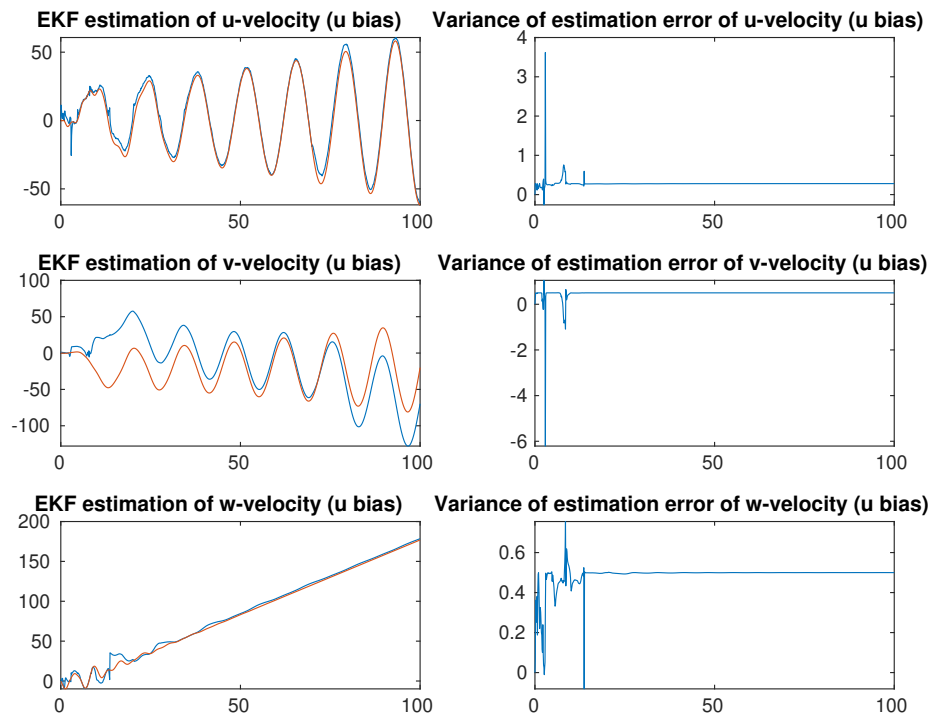


FIGURE 5.2: EKF estimation of velocity components and variance of estimation error in the presence of u velocity component bias

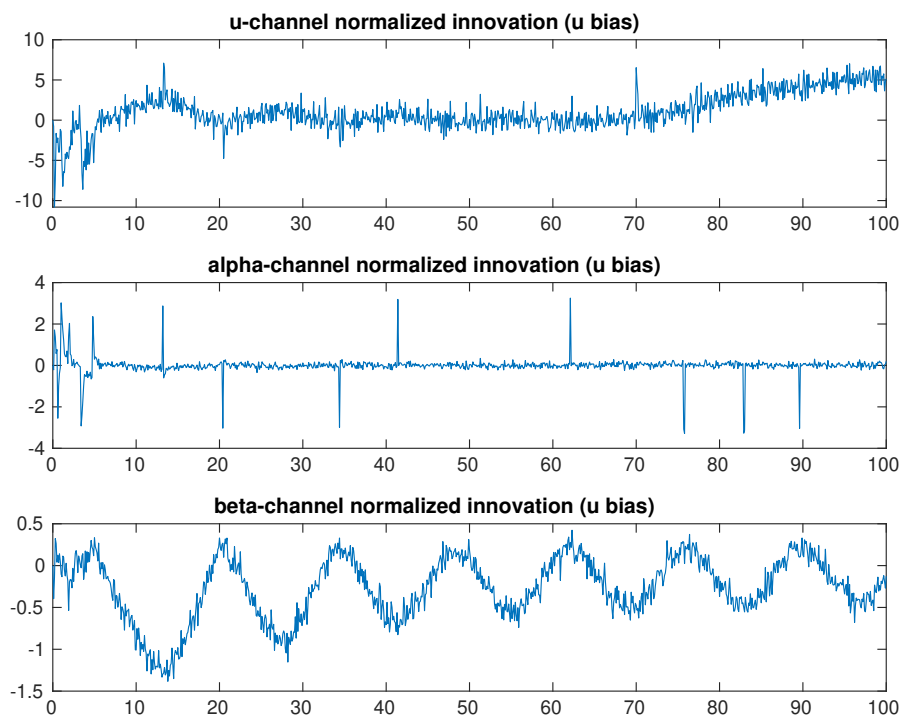


FIGURE 5.3: Innovation vector components in the presence of u velocity component bias

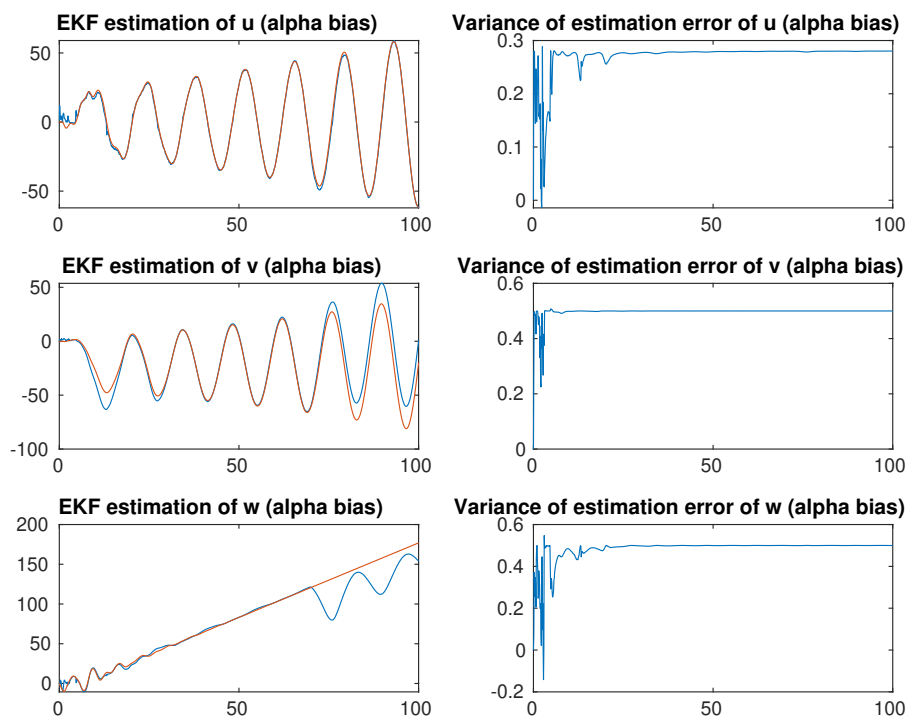


FIGURE 5.4: EKF estimation of velocity components and variance of estimation error in the presence of alpha bias

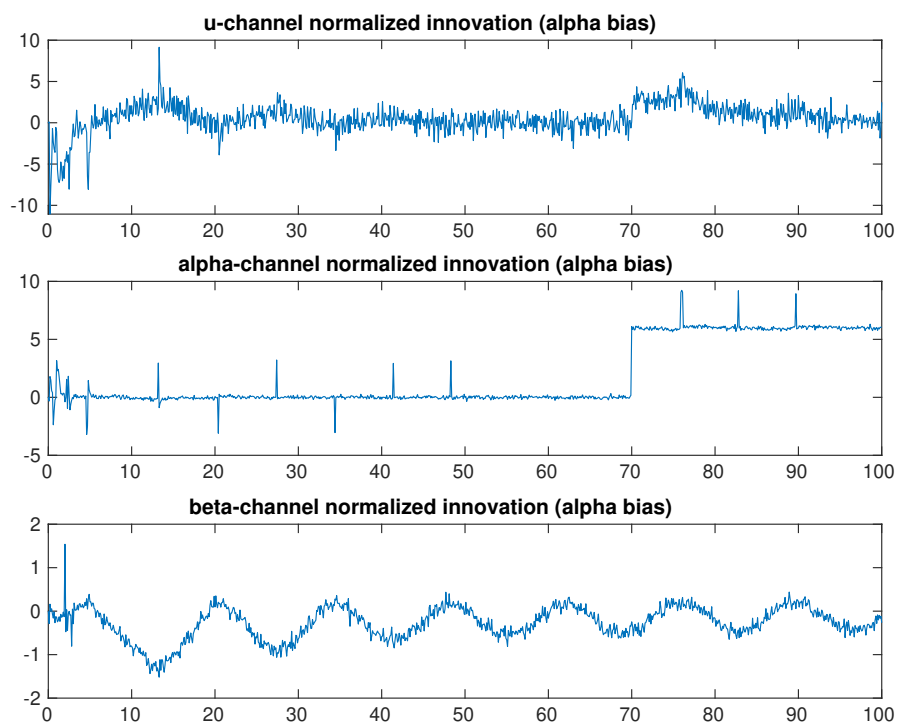


FIGURE 5.5: Innovation vector components in the presence of alpha bias

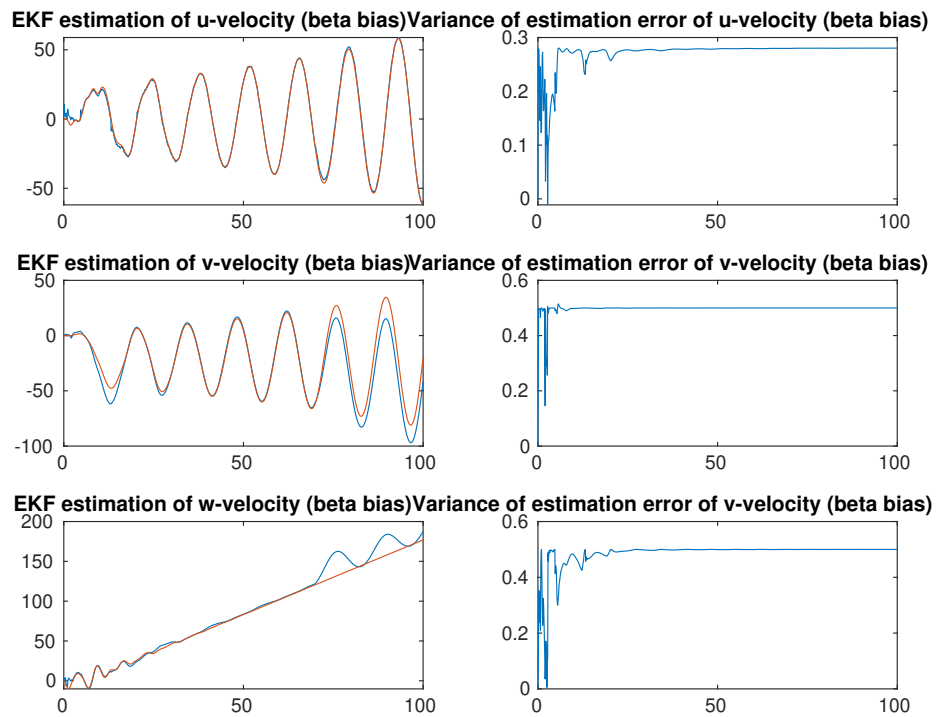


FIGURE 5.6: EKF estimation of velocity components and variance of estimation error in the presence of beta bias

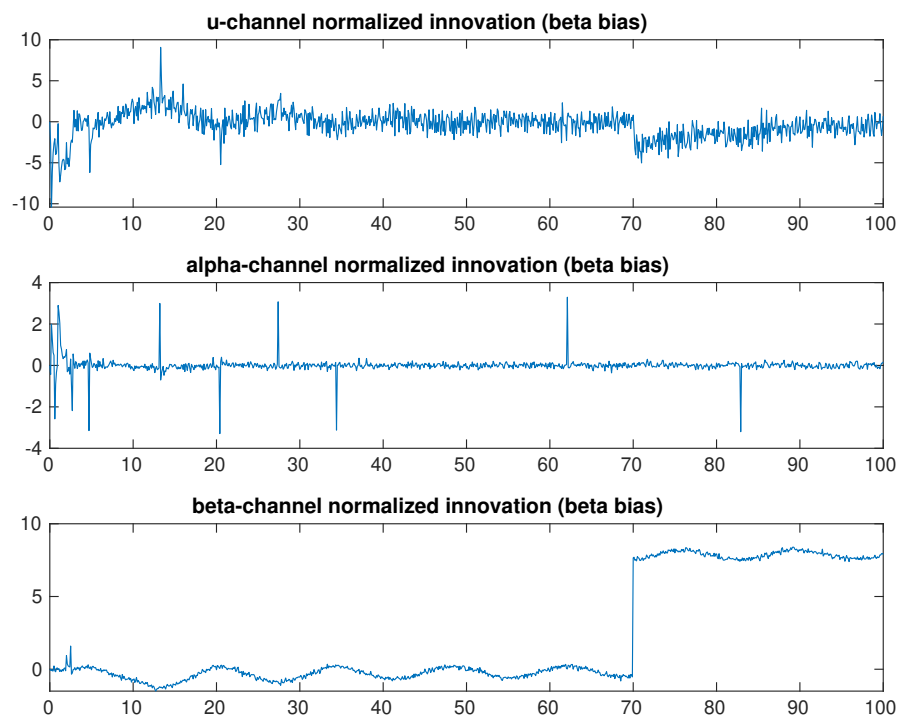


FIGURE 5.7: Innovation vector components in the presence of beta bias

Chapter 6

Conclusion

In conclusion, the design and the verification of the correct functioning of the EKF for estimation of UAV flight parameters, which is of utmost importance for flight safety, has been successfully carried out in this project. The model has proved to accurately approximate the true state of the aircraft as simulated through Matlab when tested within a faultless environment, overcoming also the initial error conditions, thus verifying its robustness against this stage of the algorithm.

Finally, the employment of the innovation step of the Extended Kalman Filter algorithm in order to detect faults in the sensor measurement system led to the diagnosis of such flaws with a high level of reliability, certifying that it can be used as an inexpensive and trustworthy tool in the prevention of defective sensors affecting the approximation of the actual state of the aircraft, which is key to the success of the aircraft mission.

Bibliography

- [1] Paul F. Bala, Edgars A. Kupcis, and William B. Fisher. *Aircraft stall warning system*. Mar. 1990. URL: <https://www.google.com/patents/US4908619>.
- [2] R. E. Kalman. "A New Approach to Linear Filtering and Prediction Problems". In: *Journal of Basic Engineering* 82.1 (Mar. 1960), pp. 35–45. ISSN: 0021-9223. DOI: 10.1115/1.3662552. eprint: https://asmedigitalcollection.asme.org/fluidsengineering/article-pdf/82/1/35/5518977/35_1.pdf. URL: <https://doi.org/10.1115/1.3662552>.
- [3] E. Wan. "Sigma-Point Filters: An Overview with Applications to Integrated Navigation and Vision Assisted Control". In: *2006 IEEE Nonlinear Statistical Signal Processing Workshop*. 2006, pp. 201–202.
- [4] F. Caliskan and C. Hacizade. "Sensor and Actuator FDI Applied to an UAV Dynamic Model". In: (). DOI: 10.3182/20140824-6-ZA-1003.01013. URL: <https://doi.org/10.3182/20140824-6-ZA-1003.01013>.
- [5] Chingiz Hajiyev and Fikret Caliskan. *Fault Diagnosis and Reconfiguration in Flight Control Systems*. Jan. 2003. ISBN: 1402076053. DOI: 10.1007/978-1-4419-9166-9.
- [6] Hajiyev Chingiz and Caliskan Fikret. "Sensor and control surface/actuator failure detection and isolation applied to F-16 flight dynamic". In: *Aircraft Engineering and Aerospace Technology* 77.2 (Jan. 2005), pp. 152–160. ISSN: 0002-2667. DOI: 10.1108/00022660510585992. URL: <https://doi.org/10.1108/00022660510585992>.
- [7] Halil Soken, Chingiz Hajiyev, and Shin-ichiro Sakai. "Robust Kalman filtering for small satellite attitude estimation in the presence of measurement faults". In: *European Journal of Control* 20 (Jan. 2013). DOI: 10.1016/j.ejcon.2013.12.002.
- [8] Lennon Cork, Rodney Walker, and Shane Dunn. "Fault Detection, Identification and Accommodation Techniques for Unmanned Airborne Vehicles". In: (Jan. 2005).
- [9] Fikret Caliskan and Chingiz Hajiyev. "A review of in-flight detection and identification of aircraft icing and reconfigurable control". In: *Progress in Aerospace Sciences* 60 (July 2013), pp. 12–34. DOI: 10.1016/j.paerosci.2012.11.001.
- [10] W. Phillips and B. Santana. "Aircraft Small-Disturbance Theory with LongitudinalLateral Coupling". In: *Journal of Aircraft - J AIRCRAFT* 39 (Nov. 2002), pp. 973–980. DOI: 10.2514/2.3050.
- [11] R.C. Nelson. *Flight Stability and Automatic Control*. McGraw-Hill aerospace science & technology series. McGraw-Hill Education, 1998. ISBN: 9780070462731. URL: <https://books.google.es/books?id=Z41TAAAMA AJ>.
- [12] Arthur Gelb. *Applied optimal estimation*. MIT press, 1974.

-
- [13] J.L. Crassidis and J.L. Junkins. *Optimal Estimation of Dynamic Systems*. Chapman & Hall/CRC Applied Mathematics & Nonlinear Science. CRC Press, 2004. Chap. 5. ISBN: 9780203509128. URL: <https://books.google.es/books?id=EeSQjQfJgkUC>.
- [14] M. Boutayeb, H. Rafaralahy, and M. Darouach. "Convergence analysis of the extended Kalman filter used as an observer for nonlinear deterministic discrete-time systems". In: *IEEE Transactions on Automatic Control* 42.4 (1997), pp. 581–586.
- [15] William Gracey. "Summary of methods of measuring angle of attack on aircraft". In: 1958.
- [16] Borja Martos and David Rogers. "Low Cost Accurate Angle of Attack System". In: Jan. 2017. DOI: [10.2514/6.2017-1215](https://doi.org/10.2514/6.2017-1215).
- [17] Stephen Whitmore, Roy Davis, and John Fife. "In-flight demonstration of a Real-Time Flush Airdata Sensing (RT-FADS) system". In: *Journal of Aircraft* 33 (Nov. 1995). DOI: [10.2514/3.47043](https://doi.org/10.2514/3.47043).
- [18] T. McDevitt and Kevin Owen. "An Optical Angle of Attack Sensor". In: vol. 5. Oct. 1989, pp. 113–124. DOI: [10.1109/ICIASF.1989.77664](https://doi.org/10.1109/ICIASF.1989.77664).
- [19] Dietrich Fischenberg. "A Method to Validate Wake Vortex Encounter Models from Flight Test Data". In: vol. 4. Sept. 2010.